

Populations of X-ray binaries and the dynamical history of their host galaxies

Kinwah Wu

Research Centre for Theoretical Astrophysics, School of Physics,
University of Sydney, NSW 2006, Australia, and
Mullard Space Science Laboratory, University College London,
Holmbury St Mary, Surrey RH5 6NT, United Kingdom
e-mail: kw@mssl.ucl.ac.uk

February 1, 2008

Abstract

The observed luminosity distributions of X-ray sources indicate the presence of several populations of X-ray binaries in the nearby galaxies. Each population has its formation and evolutionary history, depending on the host environment. The features seen in the $\log N(>S) - \log S$ curves for different types of galaxies and for different galactic components can be reproduced by a birth-death model, in which the lifespans of the binaries are inversely proportional to their X-ray brightness. Conversely, the dynamical history of a galaxy can be inferred from the luminosity distributions of its X-ray binary populations.

1 Introduction

X-ray binaries are powered by a compact star, which may be a neutron star or a black hole, accreting material from its companion. Systems having a massive OB companion star are called high-mass X-ray binaries (HMXBs), and systems with a low-mass companion star are known as low-mass X-ray binaries (LMXBs). In HMXBs the compact star accretes via capturing the stellar wind from its companion; mass transfer in LMXBs occurs when the companion star overflows its Roche lobe.

X-ray binaries in the active states are luminous and easily detected within the Galaxy. Many X-ray binaries were also found in nearby galaxies by the *Einstein* and *ROSAT* X-ray satellites (Fig. 1, see also e.g. Fabbiano 1995; Roberts & Warwick 2000), and recently, more are discovered by the *Chandra* X-ray observatory (see Weisskopf et al. 2000 for the description of the observatory). It is now evident that galaxies similar to our own (e.g. M31, Supper et al. 1997) normally host hundreds of active X-ray binaries. The current sample of X-ray binaries in external galaxies is sufficiently large that not only is reliable population analysis for an individual galaxy possible but we can also study their formation and evolution in different galactic environments.

In this paper we present a simple birth-death model and calculate the populations of X-ray binaries in external galaxies. We also use the model to identify the relevant processes that give rise to the features in the luminosity distributions of X-ray binaries (such as the $\log N(>S) - \log S$ curves) in different types of galaxies and in different galactic components. Here, only the basic formulation is presented and a few simple cases are shown as an illustration. Results of a more comprehensive study will be reported in Wu et al. (2001).

2 X-ray binaries in a galaxy

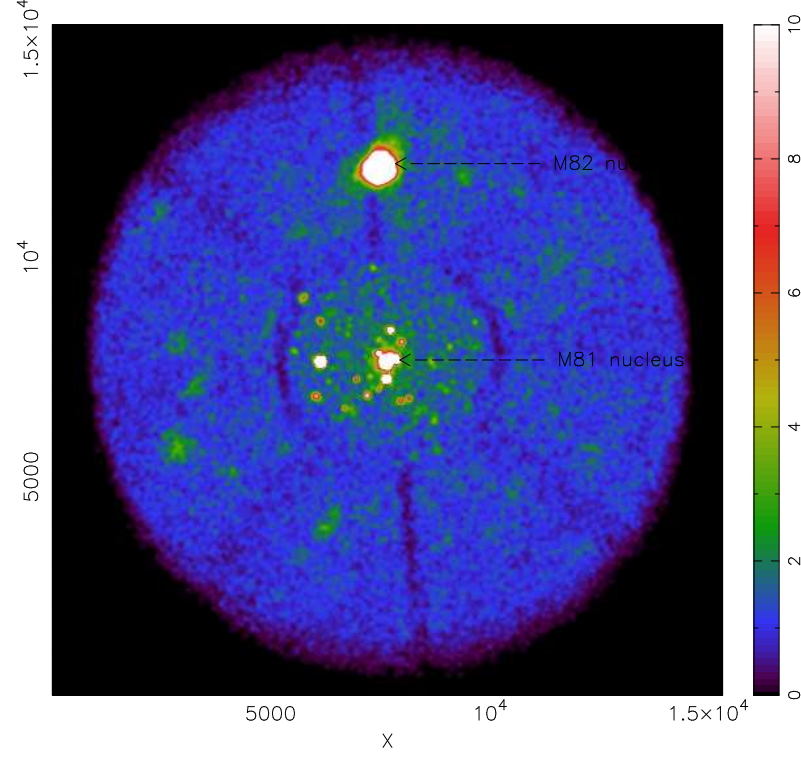


Figure 1: *ROSAT* PSPC image of the spiral galaxy M81 and the starburst galaxy M82. The brightest point sources in M81 can be easily distinguished from the background.

2.1 Accretion luminosity

The luminosity of an accreting compact star is given by

$$L_x \approx \frac{GM\dot{M}}{R} = 2.8 \times 10^{37} \left(\frac{M}{M_\odot} \right) \left(\frac{\dot{M}}{10^{-8} M_\odot \text{yr}^{-1}} \right) \left(\frac{R}{3 \times 10^6 \text{cm}} \right)^{-1} \text{erg s}^{-1}, \quad (1)$$

where G is the gravitational constant, M and R are the mass and radius of the compact star, and \dot{M} is the mass accretion rate. Typically, neutron-star binaries have luminosities $L_x \sim 10^{37} \text{erg s}^{-1}$, but the luminosities of binaries with accreting white dwarfs would not greatly exceed $10^{33} \text{erg s}^{-1}$.

The expression for L_x above is not strictly applicable to black-hole binaries, as black holes do not have a solid stellar surface that defines R . However, as accreting material attain speeds close to the light speed, c , when crossing the black-hole event horizon, we may parametrise the accreting luminosity as

$$L_x \approx \eta_{\text{bh}} \dot{M} c^2 = 5.7 \times 10^{37} \left(\frac{\eta_{\text{bh}}}{0.1} \right) \left(\frac{\dot{M}}{10^{-8} M_\odot \text{yr}^{-1}} \right) \text{erg s}^{-1}, \quad (2)$$

where η_{bh} is the efficiency. If most of the X-rays are emitted from the inner accretion disk near the last stable orbit, then $\eta_{\text{bh}} \approx 0.1$ for a Schwarzschild black hole and $\eta_{\text{bh}} \approx 0.4$ for a maximally rotating Kerr black hole.

The characteristic luminosity of neutron-star binaries can also be expressed as $L_x \approx \eta_{\text{ns}} \dot{M} c^2$, because of the tight mass distribution of neutron stars. If we assume a canonical mass of $1.5 M_\odot$ for the neutron stars, then the value of the efficiency parameter η_{ns} is about 0.3. Hence, we can adopt $L_x \approx \eta \dot{M} c^2$ (with $\eta \sim 0.1$) for both neutron-star and black-hole binaries, provided that the mass-transfer rates \dot{M} are not significantly above the Eddington limit.

2.2 Eddington limit

The infall of the material onto a compact star is opposed by the accretion-generated radiative pressure, and the accretion process is self-regulating. The limiting luminosity L_{ed} , known as the Eddington luminosity, for

spherical accretion is given by

$$L_{\text{ed}} \approx 4\pi \left(\frac{GMm_p c}{\sigma_T} \right) = 1.3 \times 10^{38} \left(\frac{M}{M_\odot} \right) \text{ erg s}^{-1}, \quad (3)$$

where m_p is the proton mass, and σ_T is the Thomson cross section. The Eddington luminosity depends linearly on the mass of the accreting star and is independent of other parameters.

As the average luminosity of an accretor would not be greater than the Eddington luminosity, the lower limit to the mass of the accretor can be constrained by the observed luminosity. Thus, we can use this as a working criterion to identify black-hole candidates. For instance, when we observe a source with X-ray luminosities greatly exceeding $2 \times 10^{38} \text{ erg s}^{-1}$, the Eddington luminosity of a $1.5\text{-}M_\odot$ compact star, we may classify it as a (candidate) black-hole system (if it is powered by accretion).

2.3 Evolution and expected lifespan

The duration of the active phase of an X-ray binary is limited by the lifespan of the companion star, and it is almost independent of the nature of the compact star. Massive OB stars have lifespans of $\sim 10^6 - 10^7 \text{ yr}$, implying that HMXBs powered by capturing the stellar wind from massive OB stars will not have a lifespan significantly longer than a few million years. The presently active HMXBs must therefore have been formed in very recent epochs.

Low-mass stars have longer lifespans and evolutionary timescales than high-mass stars, and so LMXBs can remain X-ray active over a period longer than 10^7 yr . Mass transfer in LMXBs is usually driven by Roche-lobe overflow, which is caused either by the expansion of their companion stars when they evolve towards a red-giant phase, or by orbital shrinkage, when the binaries lose orbital angular momentum.

For the first type of LMXBs, their mass-transfer rate is roughly given by $\langle \dot{M} \rangle \sim M_2/\tau_{\text{ev}}$, where M_2 is the mass of the companion star, and τ_{ev} is the evolutionary timescale. The nuclear-evolution timescale of a star depends on its mass and evolutionary stage. The lifespan of F main-sequence stars is about $5 \times 10^9 \text{ yr}$; stars later than G type take more than 10^{10} yr to evolve away from the main-sequence stage. Clearly, nuclear evolution of main-sequence stars of masses $\sim 1M_\odot$ is unable to sustain a persistent accretion luminosity $\gtrsim 10^{37} \text{ erg s}^{-1}$. Such accretion luminosities are possible for LMXBs with evolved companion stars. The duration of the red-giant phase is $\lesssim 10^7 \text{ yr}$ for low mass stars (de Loore & Doom 1992), and hence, X-ray binaries with a red-giant companion are short-lived. However, galactic stars evolve into the red-giant stage at all epochs. X-ray binaries with red-giant companions are therefore formed continually throughout the life time of a galaxy.

For the second type of LMXBs, orbital angular momentum can be extracted from the systems by emitting gravitational radiation (Paczynski 1967) or by rotational braking of the companion star via a magnetic stellar wind (Verbunt & Zwaan 1981). The timescale of orbital evolution driven by gravitational radiation is

$$\begin{aligned} t_{\text{gr}} &= \frac{5}{32(2\pi)^{8/3}} \frac{c^5}{G^{5/3}} \frac{(M_1 + M_2)^{1/3}}{M_1 M_2} P^{8/3} \\ &= 3.8 \times 10^{11} (1+q)^{1/3} q^{-1} \left(\frac{M_1}{M_\odot} \right)^{-5/3} \left(\frac{P}{1 \text{ day}} \right)^{8/3} \text{ yr} \end{aligned} \quad (4)$$

(Landau & Lifshitz 1971, see also Wu 1997), where P is the orbital period, M_1 and M_2 are the masses of the compact star and the companion star respectively, and $q (\equiv M_2/M_1)$ is the mass ratio. As the timescale of orbital shrinkage is long ($\gg 10^9 \text{ yr}$), the corresponding mass-transfer rate is not large enough to account for the observed luminosity of the X-ray binaries. The orbital evolutionary timescale for magnetic braking is

$$t_{\text{mb}} = \frac{2 \times 10^{28}}{(2\pi)^{10/3}} \frac{f^2 G^{2/3} M_\odot^{4\gamma}}{\tilde{k}^2 R_\odot^4} \frac{M_1 P^{10/3}}{(M_1 + M_2)^{1/3} M_2^{4\gamma}} \text{ sec} \quad (5)$$

$$= 4.4 \times 10^9 f^2 (1+q)^{-1/3} q^{-4\gamma} \left(\frac{\tilde{k}^2}{0.1} \right)^{-1} \left(\frac{M_1}{M_\odot} \right)^{(2-12\gamma)/3} \left(\frac{P}{1 \text{ day}} \right)^{10/3} \text{ yr} \quad (6)$$

(Verbunt & Zwaan 1981; Wu 1997). The parameters \tilde{k} and f depend on the stellar model (see Skumanich 1972), and the parameter γ is determined by the mass-radius relation ($R_2 \propto M_2^\gamma$, where R_2 is the radius of the companion). For low-mass stars, $\tilde{k}^2 \approx 0.1$, $f \sim 1$ and $\gamma \approx 1$. The mass-transfer rate is higher than that in the case of gravitational radiation, and the active phase of these X-ray binaries usually lasts $\gtrsim 10^8 \text{ yr}$.

3 Populations of X-ray binaries

In a simplistic point of view the populations of X-ray binaries in a galaxy observed at an epoch t are determined by the birth rates and the lifespans of the binaries. Assuming other factors are unimportant (for example, the two-body and three-body capture process in globular clusters, see Johnston & Verbunt 1996), we can construct a birth-death model and calculate the populations and luminosity distributions of X-ray binaries in a galaxy or in a particular galactic component.

The basic formulation is as follows. Let the number of the X-ray sources at the luminosity range $(L, L+dL)$ in a galaxy at time t be $n(L, t)dL$ and the characteristic lifespan of these sources be τ . The evolution of an X-ray binary population is governed by

$$\frac{d}{dt}n(L, t) = -k n(L, t) + f(L, t), \quad (7)$$

where $k n(L, T)$ is the death rate, the $f(L, t)$ is the birth rate, and $k^{-1} (\equiv \tau)$ is the characteristic lifespan of the sources. The number of sources with a luminosity brighter than L is simply

$$N(> L, t) = \int_L^\infty dL n(L, t). \quad (8)$$

When the functional forms of k and $f(L, t)$ are specified, Equations (7) and (8) can be solved easily.

3.1 Impulsive birth

X-ray binaries are born (i.e. become X-ray active) when mass transfer from the companion to the compact star starts; and they die when the X-ray active phase ends. Suppose that there are two channels to create X-ray binaries in a galaxy: (i) systems that are formed continuously and the mass transfer of these systems is sustained by nuclear evolution of the companion star or by the orbital evolution of the binary, and (ii) systems that are born in a recent star-formation episode. The birth rate function $f(L, t)$ thus consists of a steady (continual birth) component and an impulsive (starburst) component:

$$f(L, t) = f_o(L)[1 + a\delta(t - t_a)], \quad (9)$$

where $f_o(L)$ is the birth rate of the steady component, a is the ratio of the strength of the impulsive component to the strength of the steady component, $\delta(t - t_a)$ is the Dirac δ -function, and t_a is the time at which the starburst occurred.

The effective duration of the active phase of an X-ray binary is determined by the mass of the companion star and the mass-transfer rate, and it is approximately given by $M_2/\langle \dot{M} \rangle$. As $L_x \propto \dot{M}$, the characteristic lifespan of an X-ray binary k^{-1} can be parametrised as $k = \beta L$, where $\beta^{-1} = \tilde{\eta} \langle M_2 \rangle c^2$ and $\langle M_2 \rangle$ is the mean mass of the companion star, and $\tilde{\eta}$ is a parameter which has the same order of magnitude as the parameters η_{bh} and η_{ns} in §2. The fact that the characteristic lifespan of binaries with luminosities in the range $(L, L + dL)$ is not explicitly time-dependent allows us to integrate Equation (7) directly, yielding

$$n(L, t) = n_o(L) e^{-\beta L t} + \frac{f_o(L)}{\beta L} \left(1 - e^{-\beta L t} \right) + a f_o(L) \theta(t - t_a) e^{-\beta L (t - t_a)}, \quad (10)$$

where $\theta(t - t_a)$ is the Heaviside unit step function, and $n_o(L) \equiv n(L, 0)$ is the initial population.

If the initial population and the birth rate are power-laws of L , i.e. $n_o = n_{o*}(L/L_*)^{-\alpha_1}$ and $f_o = f_{o*}(L/L_*)^{-\alpha_2}$ (with power-law indices α_1 and α_2 respectively), then

$$\begin{aligned} N(> L, t) = & n_{o*} L_* (\beta L_* t)^{\alpha_1 - 1} \Gamma(1 - \alpha_1, \beta L t) \\ & + \frac{f_{o*}}{\beta} (\beta L_* t)^{\alpha_2} \left[\frac{1}{\alpha_2} (\beta L t)^{-\alpha_2} \left(1 - e^{-\beta L t} \right) + \frac{1}{\alpha_2} \Gamma(1 - \alpha_2, \beta L t) \right] \\ & + a f_{o*} L_* [\beta L_* (t - t_a)]^{\alpha_2 - 1} \Gamma(1 - \alpha_2, \beta L (t - t_a)) \theta(t - t_a), \end{aligned} \quad (11)$$

where L_* is a lower cut-off luminosity, and $\Gamma(\alpha, x)$ is the incomplete gamma function. In the limits of $f_{o*} \rightarrow 0$ (i.e. all the sources are primordial) the X-ray binary population has a distribution similar to the Schechter (1976) analytic luminosity function for galaxies in clusters. The same distribution is also obtained when $(f_{o*}/\beta L_*) \gg n_{o*}$ and $a\beta L_* \gg 1$ (i.e. most of the binaries were born in a recent starburst). The difference between the Schechter (1976) luminosity function and the distribution that we obtain here is that in the latter case the luminosity break is time dependent — it is caused by the aging of the source population when it is not replenished.

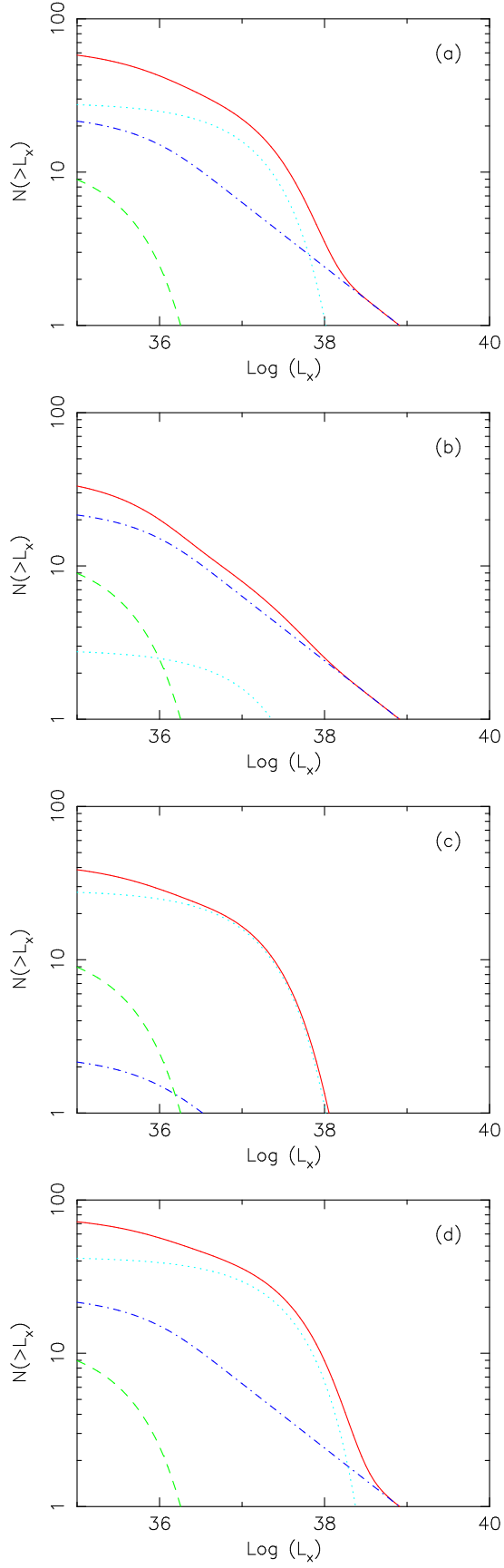


Figure 2: Luminosity distributions of X-ray binaries in model galaxies for the impulsive-birth model. In the calculations we assume an age of 15 Gyr for the Universe. We also define two parameters $\lambda_c \equiv (f_{o*}/n_{o*}\beta L_*)$ and $\lambda_a \equiv (af_{o*}/n_{o*})$ to specify the relative strength of the continuous and the impulsive birth models. (a) $\lambda_c = 0.5$, $\lambda_a = 10$ (b) $\lambda_c = 10$, $\lambda_a = 0.5$ (c) $\lambda_c = 0.5$, $\lambda_a = 100$ (d) $\lambda_c = 10$, $\lambda_a = 100$

3.2 Cyclic generation

In reality, star formation may not be a single event. For example, when two galaxies are orbiting around each other, periodic starbursts are induced by orbital interaction. In this case, the birth term $f(L, t)$ has a periodic (starburst) component superimposed on a steady background:

$$f(L, t) = f_o(L) [1 + b \cos \omega t] , \quad (12)$$

where $2\pi/\omega$ is the characteristic timescale of the cycle. It follows that the population of X-ray binaries at time t is

$$n(L, t) = n_o(L) e^{-\beta L t} + \frac{f_o(L)}{\beta L} \left(1 - e^{-\beta L t} \right) + \frac{b f_o(L)}{\beta L} \left[\left(1 - e^{-\beta L t} \right) + \frac{(\beta L)^2}{(\beta L)^2 + \omega^2} \left(1 - \cos \omega t - \frac{\omega}{\beta L} \sin \omega t \right) \right] , \quad (13)$$

and the number of systems brighter than L is

$$N(> L, t) = n_{o*} L_* (\beta L_* t)^{\alpha_1 - 1} \Gamma(1 - \alpha_1, \beta L t) + \frac{f_{o*}}{\beta} (\beta L_* t)^{\alpha_2} \left[\frac{1}{\alpha_2} (\beta L t)^{-\alpha_2} \left(1 - e^{-\beta L t} \right) - \Gamma(1 - \alpha_2, \beta L t) \right] + \frac{b f_{o*}}{\beta} (\beta L_* t)^{\alpha_2} \left\{ \left[\frac{1}{\alpha_2} (\beta L t)^{-\alpha_2} \left(1 - e^{-\beta L t} \right) + \Gamma(1 - \alpha_2, \beta L t) \right] + \left[I(\alpha_2 - 1; \omega t, \beta L t) (1 - \cos \omega t) - I(\alpha_2; \omega t, \beta L t) (\omega t) \sin \omega t \right] \right\} . \quad (14)$$

The integral $I(\alpha; \omega t, \beta L t)$ above is defined as

$$I(\alpha; \omega t, \beta L t) \equiv \int_{\beta L t}^{\infty} dx \frac{x^{-\alpha}}{x^2 + (\omega t)^2} , \quad (15)$$

and it has exact analytic form for integer α . The periodic component may introduce ripple-like features in the luminosity function, hence makes the $\log N(>S) - \log S$ curves deviate from a simple or a broken power law.

3.3 Other issues

3.3.1 Neutron-star binaries

The model above has not accounted for the fact that the persistent luminosity of neutron-star binaries cannot exceed the Eddington limit of a $1.5\text{-}M_{\odot}$ accretor. The luminosities of black-hole binaries are less restrictive, as there is no practical mass limit for black holes. A more proper treatment requires the populations of neutron-star and black-hole binaries be calculated separately. Although Equation (7) is applicable for both classes of objects, the corresponding expressions for $N(> L)$ are not identical. For a population of X-ray binaries with a cutoff luminosity at L_{ed} , $N(> L)$ is given by

$$N(> L, t) = \int_L^{L_{\text{ed}}} dL n(L, t) . \quad (16)$$

The tight mass distribution of neutron stars together with the presence of a luminosity limit will produce a spike at L_{ed} in the (differential) luminosity function $n(L)$, and hence a cut-off in the observed $\log N(>S) - \log S$ curve.

The strength of the spike in $n(L)$ is time-dependent. If all the neutron-star binaries in the galaxy were born at the same episode, because the systems with high mass-transfer rates cease to be active first and then those with lower mass-transfer rates, the spike will gradually decrease, on a timescale

$$t_{\text{sp}} \lesssim \frac{\langle M_2 \rangle}{\dot{M}_{\text{ed}}} \quad (17)$$

$$\approx 1.3 \times 10^8 \frac{M_2}{M_{\text{ns}}} \text{ yr} , \quad (18)$$

where \dot{M}_{ed} and M_{ns} is the Eddington mass-accretion rate and the mass of neutron stars respectively. For galaxies with star-formation activity occurred more than 10^8 yr ago, the spike has already degraded so substantially

that it may not be detected easily (Wu et al. 2001). The spike is, however, prominent for galaxies with violent starburst activity in the near past ($\lesssim 10^7$ yr), or if the neutron-star binaries are formed continuously.

3.3.2 Transient sources

The total duration of the X-ray active phases of transients is only some fraction of their lifespans. The parameter k is therefore not exactly equal to \dot{M}/\dot{M}_2 , but is proportional to it. As a first approximation, we may use an effective factor ξ to specify the fractional time at which the source is X-ray active, i.e. $k = \beta L/\xi$. If ξ does not depend on L explicitly, the solution to Equation (7) preserves its form. Otherwise, the solution and hence the luminosity functions are modified.

It is worth noting that in addition to different fractional time ξ for their X-ray active phases, the transients and persistent sources have different discovery probabilities. This could complicate the calculations of the source populations and luminosity functions. Here, we have omitted the transient effects for simplicity, but one must bear in mind that the effects might be important.

4 X-ray sources in external galaxies

Since 1999, *Chandra* has obtained high-resolution images of a number of nearby galaxies. These include the ellipticals M84 (NGC 4374) (Finoguenov & Jones 2001) NGC 4967 (Sarazin, Irwin & Bregman 2000), and Cen A (Kraft et al. 2000), the lenticulars NGC 1553 (Blanton, Sarazin & Irwin 2001) and NGC 1291 (Irwin, Bregman & Sarazin 2001), the spirals M31 (NGC 224) (Garcia et al. 2000), M81 (NGC 3031) (Tennant et al. 2001), M101 (NGC 5457) (Pence et al. 2001) and the Circinus galaxy (Sambruna et al. 2001), and the irregular starburst galaxy M82 (NGC 3034) (Matsumoto et al. 2001), and the mergers NGC 4038/4039 (Fabbiano, Zezas & Murray 2001). The *Chandra* observations show more than a hundred bright X-ray sources (with $L_x > 10^{36}$ erg s $^{-1}$) in the field each of these galaxies. While some of the bright sources are foreground stars and background AGN, the majority are probably X-ray binaries within the galaxies. The observations also indicate that the brightest sources in the early-type galaxies are generally brighter than their counterparts in the spiral galaxies, if the galactic nuclei are excluded.

4.1 log N(>S) – log S curve

The log N(>S) – log S curves of the *Einstein* and *ROSAT* sources in spiral galaxies are in general adequately fitted by a power law (see Fabbiano 1995). However, for the galaxies with a sufficiently large number of sources discovered (\gtrsim a few tens), the log N(>S) – log S curves are found to deviate significantly from a single power law, e.g. M31 (see Supper et al. 1997) and M101 (Fig. 3, left panel; see also Wang, Immler & Pietsch 1999). A broken power law is often required in order to fit the log N(>S) – log S curves. The break L_c is located at \sim a few $\times 10^{37}$ erg s $^{-1}$ (see e.g. M31, Supper et al. 1997; Shirey et al. 2001).

The *Chandra* observations confirm the presence of the broken power-law in the log N(>S) – log S curves of X-ray sources in spiral galaxies (e.g. M81, Tennant et al. 2001). They also verify that the broken power law is present in the log N(>S) – log S curves for early-type galaxies, e.g. NGC 4697 (Sarazin, Irwin & Bregman 2000), NGC 1553 (Fig. 3, right panel) and M84 (A. Finoguenov, private communication). The fact that a luminosity break is found in both the cases of early- and late-type galaxies suggests that the break may be universal. A possible explanation is that the luminosity break is caused by a population of neutron-star binaries which have super-Eddington mass-transfer rates. These neutron-binaries would have X-ray luminosities roughly about 2×10^{38} erg s $^{-1}$, the Eddington luminosity of the $1.5\text{-}M_\odot$ accretors. If the location of the luminosity break is the same for all galaxies, it can be used as a distance indicator (Sarazin, Irwin & Bregman 2000).

However, when the X-ray sources in the disk and in the bulge of M81 are considered separately, very different log N(>S) – log S curves are obtained (Fig. 4, Tennant et al. 2001). The luminosity break is obvious in the log N(>S) – log S curve of the bulge sources, but the log N(>S) – log S curve of the disk sources is a single power law. Interestingly, the power-law slope of the disk sources is similar to that of the bulge sources below the luminosity break.

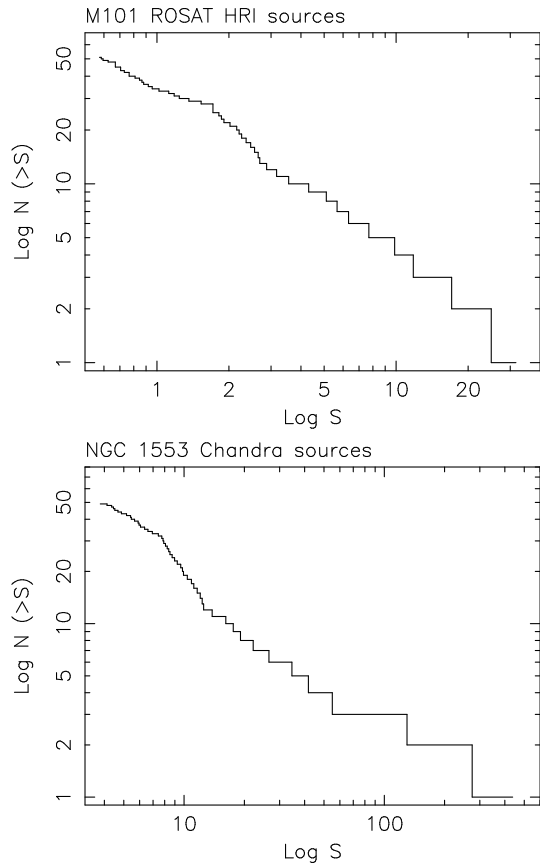


Figure 3: (Left) The $\log N(>S) - \log S$ curve of the *ROSAT* HRI sources in M101 (NGC 5457). The data are taken from Table 3 in Wang, Immler & Pietsch (1999). The unit of S is counts per kilo-second. For an assumed distance of 7.7 Mpc to the galaxy, 1 unit corresponds roughly to a luminosity of $2.8 \times 10^{38} \text{ erg s}^{-1}$ at 0.5–2.0 keV (1 cts ks^{-1} is approximately $4.0 \times 10^{-14} \text{ erg s}^{-1}$). (Right) The $\log N(>S) - \log S$ curve of the *Chandra* sources in NGC 1553. The data are taken from Table 1 in Blanton, Sarazin & Irwin (2000). The unit of S is counts per 10 kilo-second. The conversion between count rate and the unabsorbed X-ray luminosity is $4.91 \times 10^{41} \text{ erg cts}^{-1}$ at the 0.3–10 keV (see Blanton, Sarazin & Irwin 2000 for details).

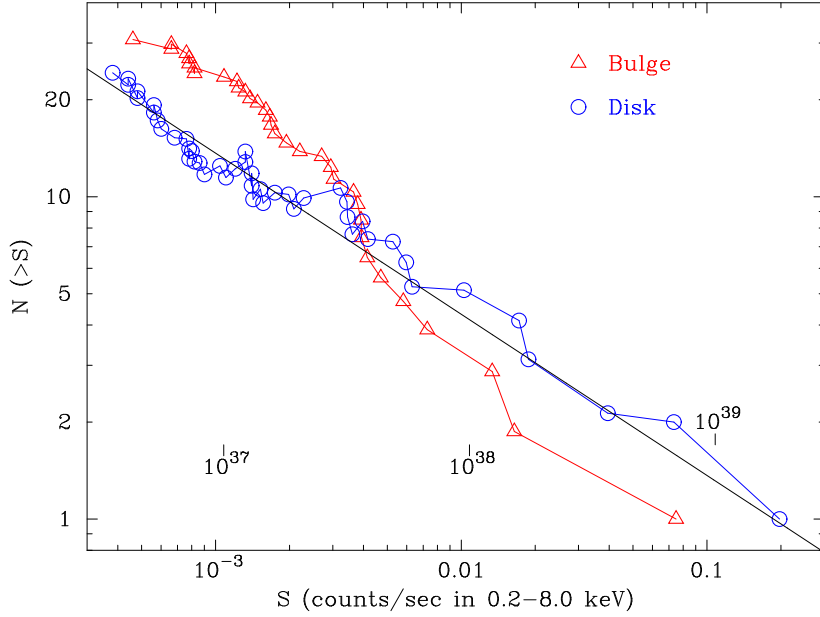


Figure 4: The $\log N(>S) - \log S$ curves of the disk and bulge sources of M81 observed by *Chandra*. The sources are background subtracted with the $\log N(>S) - \log S$ distribution of the background taken from *Chandra* calibration observation of CRSS J0030.5+2618. Adopted from Tennant et al. (2001).

4.2 Dynamical evolution of the host galaxy

The absence of the break in the $\log N(>S) - \log S$ curve of the disk sources in M81 is inconsistent with the proposition that the luminosity break is universal for all galaxies. The locations of the breaks at different luminosities for early- and late-type galaxies (cf. M81 and NGC 4697, see Tennant et al. 2001 and Sarazin, Irwin & Bregman 2000 respectively) suggest that the natures of the breaks are different for galaxies with different Hubble types. We propose that for some galaxies the luminosity break is determined by the formation and evolutionary history of the populations of X-ray binaries in the galaxy. The different morphologies for the $\log N(>S) - \log S$ curves for the disk and bulge sources in the spiral galaxies reflect the different star-formation histories for the galactic components and the different evolutionary paths of their X-ray binary populations.

We interpret the absence of the luminosity break in the $\log N(>S) - \log S$ curve for disk sources in the spiral galaxy M81 as being a consequence of a continuous, smooth star-formation process. In normal spiral galaxies, star formation is triggered by compression of gas when the density wave sweeps across the galactic disk. The star-formation process is continuous and is relatively smooth (in comparison with the environment in starburst galaxies and mergers). As the X-ray binaries are formed continually in the spiral arms, the bright sources are dominated by young HMXBs with substantial proportion of black-hole binaries. The disk sources may also consist of two types of older LMXBs: one with their companion stars evolving into the red-giant phase, another one with their orbital separation sufficiently shrunk that the systems become semi-detached. Many of these LMXBs may contain accreting neutron stars. However, if the young HMXBs dominate the total population, there will not be a prominent luminosity break in the $\log N(>S) - \log S$ curve.

Formation of X-ray binaries in a galactic component is continuous if the galaxy is undisturbed. In this case, the population is dominated by LMXBs which are formed via processes the same as those of the LMXBs in the galactic disk. If the bulge is disturbed, e.g. by tidal interaction with another galaxy, a starburst is triggered by a sudden infall of gas, and a new population of stars as well as X-ray binaries are formed. As shown in §3.1, such an impulsive formation can produce a prominent luminosity break in the $\log N(>S) - \log S$ curve, and the location of the break. When the population of the X-ray binaries ages, the break migrates to low luminosities, thus marking the look-back time of the catastrophic star-forming episode.

Interestingly, the luminosity break in the $\log N(>S) - \log S$ curve for the sources in the ellipticals (e.g. NGC 4697) seems to occur at a higher luminosity than that for the bulge sources in the spirals (e.g. M31 and M81) (A. F. Tennant and D. A. Swartz, private communication). If luminosity breaks are created solely by the aging of X-ray binary populations, the break seen in the $\log N(>S) - \log S$ curves of the *Chandra* sources in the

early-type galaxies indicate that these galaxies had experienced some, possibly violent, star-formation activity in the very near past.

However, this interpretation must be taken with caution. As pointed out in §3.3.1, the tight mass distribution of neutron stars together with the presence of an Eddington limit for each accretor could produce a spike in $n(L)$ and hence a luminosity cut off in $N(>L)$. A substantial proportion of neutron-star binaries in the X-ray binary population can also cause a luminosity break in the $\log N(>S) - \log S$ curve. The break caused by a population of neutron-star binaries with massive companions is expected to be located at $L_x \approx 2 \times 10^{38} \text{ erg s}^{-1}$, the Eddington luminosity of a $1.5\text{-}M_\odot$ accretor. Its strength will decrease on a timescale $\lesssim 10^8 \text{ yr}$, if there is no replenishment of the systems. As the luminosity breaks seen in the $\log N(>S) - \log S$ curves of the sources in the bulge of the spirals scatter over a range of luminosities, they are unlikely to be all due to a population of accreting neutron stars. It is, however, possible that the breaks in the $\log N(>S) - \log S$ curves of the early-type galaxies are caused by a population of neutron-star binaries with high mass-transfer rates.

4.3 Super-Eddington sources

Although super-Eddington sources seem to be more abundant in the early-type galaxies, given the different stellar contents in the galaxies, the excess of bright sources in the early-type galaxies is yet to be confirmed. The finding that the brightest sources in the spirals tend to be located in the disk (e.g. in M81, Tennant et al. 2001) implies that the disk sources are probably young systems. This also implies that the brightest sources in the spiral galaxies and the brightest sources in the early-type galaxies may not form in the same way. The population of bright sources in the arms of the spiral galaxies are dominated by HMXBs, in which the mass donors are young massive OB stars with strong winds; while the population of bright sources in the ellipticals and lenticulars are LMXBs, with a red-giant companion overflowing its Roche lobe.

Despite the conventional scenario that X-ray sources in galaxies are mostly X-ray binaries, the super-Eddington sources may be an inhomogeneous class of exotic objects: hypernovae, supernovae, supersoft sources, intermediate-mass black holes, large clusters of massive OB stars, etc. These sources have not been included in our calculations presented above, and hence the results that we obtain may not truly reflect the real populations of X-ray sources in the galaxies. However, in order to take into account these objects, one must have some working models for their formation and evolution, which are unfortunately not available at present. On the bright side, if we accept the simple model in §3 by faith, we can explain the basic features in the $\log N(>S) - \log S$ curves, and also use the observed populations of X-ray sources to probe the dynamical history of their host galaxy in the near past.

5 Summary

We have constructed a simple birth-death model and calculated the luminosity function of X-ray binaries in external galaxies. The model reproduces the features, such as the luminosity break, in the $\log N(>S) - \log S$ curves of spiral galaxies. By assuming a continual formation process, the model also explains the absence of a luminosity break for the disk sources in M81. The location of the luminosity break depends on the look-back time of the previous starburst/star-formation activity, and so it can be used to probe the dynamic history of the host environment of the X-ray sources.

Acknowledgements

I thank Prof. Don Melrose for generously providing me with the research support in the last eight years. This work summarises a talk presented at the Melrose Festschrift in honour of his 60th birthday. The ideas presented in this work were developed during the discussions with Drs Richard Hunstead, Allyn Tennant, Douglas Swartz, Helen Johnston, Kajal Ghosh and Roberto Soria, and credits to the author, if any, should also belong to all of them. I thank Dr Alex Finoguenov for correspondence and for showing me the luminosity function of the *Chandra* sources in M84 before publication, Dr Roberto Soria for the *XMM-Newton* sources in M31, and Dr Kajal Ghosh for the *ROSAT* image of M81 and M82 (Fig. 1). I would also thank Drs Martin Weisskopf and Allyn Tennant for funding my visits to NASA-MSFC, where this work was started. This work is partially supported by an ARC Australian Research Fellowship and by a University of Sydney Sesqui R&D Grant.

Reference

- Blanton, E. L., Sarazin, C. L., Irwin, J. A. 2001, *ApJ*, 552, 106
- de Loore, C. W. H., Doom, C. 1992, *Structure and Evolution of Single and Binary Stars* (Dordrecht: Kluwers Academic Press)
- Fabbiano, G. 1995, in *X-ray Binaries*, eds. W. H. G. Lewin, J. van Paradijs and E. P. J. van den Heuvel (Cambridge: Cambridge University Press), 390
- Fabbiano, G., Zezas, A., Murray, S. S. 2001, *ApJ*, 554, 1035
- Finoguenov, A., Jones, C. 2001, *ApJ*, 547, L107
- Garcia, M. R., et al. 2000, *ApJ*, 537, L23
- Garcia, M. R., et al. 2001, in *Galaxies at the Highest Angular Resolution*, ASP Conf. Ser., in press (astro-ph/0012387)
- Irwin, J. A., Bregman, J. N., Sarazin, C. L. 2001, preprint
- Johnston, H. M., Verbunt, F. 1996, *A&A*, 312, 80
- Kraft, R. P., et al. 2000, *ApJ*, 531, L9
- Landau, L. D., Lifshitz, E. M. 1971, *The Classical Theory of Field* (Oxford: Pergamon Press)
- Matsumoto, H., et al. 2001, *ApJ*, 547, L25
- Paczynski, B. 1971, *Acta Astron.*, 17, 287
- Pence, W. D., Snowden, S. L., Mukai, K., Kuntz, K. D. 2001, preprint (astro-ph/0107133)
- Roberts, T. R., Warwick, R. S. 2000, *MNRAS*, 315, 98
- Sambruna, R. M., et al. 2001, *ApJ*, 546, L9
- Sarazin, C. L., Irwin, J. A., Bregman, J. N. 2000, *ApJ*, 544, L101
- Schechter, P. 1976, *ApJ*, 203, 297
- Shirey, R., et al. 2001, *A&A*, 365, L195
- Skumanich, A. 1972, *ApJ*, 171, 565
- Supper, R., et al. 1997, *A&A*, 317, 328
- Tennant, A. F., Wu, K., Ghosh, K. K., Kolodziejczak, J. J., Swartz, D. A. 2001, *ApJ*, 549, L43
- Verbunt, F., Zwaan, C., 1981, *A&A*, 100, L7
- Wang, Q. D., Immler, S., Pietsch, W. 1999, *ApJ*, 523, 121
- Weisskopf, M. C., Tananbaum, H. D., Van Speybroeck, L. P., O'Dell, S. L. 2000, *Proc. SPIE*, 4012, 2
- Wu, K. 1997, in 'Accretion Phenomena and Related Outflows', eds. D. T. Wickramasinghe, G. V. Bicknell and L. Ferrario, ASP Conf. Ser., 121, 283
- Wu, K., Tennant, A. F., Swartz, D. A., Ghosh, K. K., Hunstead, R. W. 2001, *ApJ*, submitted